ELSEVIER

QM/MM and SCRF studies of the ionization state of 8-methylpterin substrate bound to dihydrofolate reductase: Existence of a low-barrier hydrogen bond

Peter L. Cummins* and Jill E. Gready*

**Computational Molecular Biology and Drug Design Group, John Curtin School of Medical Research, Australian National University, Canberra, Australia*

Using combined semiempirical quantum mechanics and molecular mechanics (QM/MM) and ab initio self-consistent reaction field (SCRF) calculations, we determined that a low-barrier hydrogen bond (LBHB) is formed when the mechanism-based substrate 8-methylpterin binds to dihydrofolate reductase (DHFR). The substrate initially was assumed bound either in the ion-pair form corresponding to N3-protonated substrate hydrogen (H) bonded to the unprotonated (carboxylate) of the conserved Glu30 residue in the active site, or in the neutral-pair form corresponding to unprotonated substrate H bonded to the neutral (carboxylic acid) form of Glu30. The free energy of interaction of these H-bonded systems with the protein/solvent surroundings was computed using a coordinate-coupled free energy perturbation (FEP) method implemented within the molecular dynamics (MD) simulation scheme and using a semiempirical (PM3) QM/MM force field. The free energy obtained from the QM/MM force-field simulations corresponds most closely with the corresponding free energy component obtained from HF/6-31G SCRF calculations using a value of 2 for the dielectric constant (ϵ) for the solvated protein. Calculations were performed at levels ranging from HF/6-31G to MP2/6-31G* to B3LYP/6-31+G**, with varying dielectric constants. The energy-minimized path for motion of the proton in the H bond along a one-dimensional reaction coordinate was calculated at HF/6-31G, HF/6-31G* ($\epsilon = 1$) and B3LYP/6-31G* ($\epsilon = 2$) levels. These calculations identified a second neutral-pair complex, involving the 2-amino group of substrate, which also interacts with Glu30, which is lower in energy than the ion-pair form. A harmonic vibrational analysis shows that the first vibrational state appears to lie near or above the TS connecting potential energy minima corresponding to the two neutral-pair configurations, thus indicating an LBHB. Consequently, the H-bonded system will have a significant probability of being found in the ion-pair form, in agreement with experimental spectral studies indicating an enzyme-bound cation and suggesting that the LBHB would activate substrate towards hydride-ion transfer from NADPH.*

Keywords: QM/MM, SCRF, free energy, hydrogen bonds, ion pair, low-barrier hydrogen bond, dielectric constant, dihydrofolate reductase

INTRODUCTION

In an effort to elucidate the catalytic mechanism of dihydrofolate reductase (DHFR), we used a range of computational methods including molecular dynamics and free energy perturbation (MD/FEP) and combined quantum mechanical and molecular mechanical (QM/MM) methods to study the hydride-ion transfer between NADPH and the model substrate, 8-methylpterin.[1–3] 8-Methylpterin is the lead compound of a class of novel mechanism-based substrates[4–7] and inhibitors of DHFR that bind the active site in a manner similar to the natural substrates, folate and dihydrofolate. That is, they are assumed hydrogen (H) bonded to a conserved acidic residue (Asp/Glu) in the active site of DHFR. Figure 1 shows

Corresponding author: J.E. Gready, CMBDDG, John Curtin School of Medical Research, Australian National University, P.O. Box 334, Canberra ACT 2601, Australia. Tel.: 61-2-6279-8304; fax: 61-2-6249-0415.

E-mail address: jill.gready@anu.edu.au (J.E. Gready)

Journal of Molecular Graphics and Modelling 18, 42–49, 2000

655 Avenue of the Americas, New York, NY 10010

1093-3263/00/$–see front matter
PII S1093-3263(00)00034-6

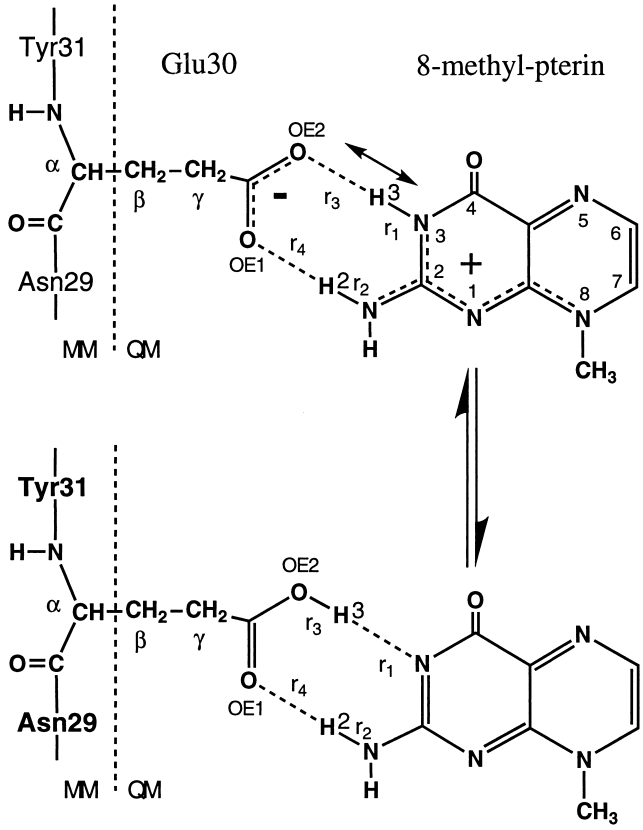

Figure 1. H bonding between the 8-methylpterin substrate and side chain of Glu30 in avian DHFR, for both ion-pair and neutral-pair complexes. The systems are shown partitioned into QM and MM regions for the QM/MM calculation of the interaction free energy by the FEP/MD method, with the reaction coordinate for the coordinate coupling shown by the arrow.

8-methylpterin H bonded to the Glu30 residue of avian (vertebrate) DHFR as the N3 protonated (ion-pair) and OE2 protonated (neutral) forms. Note that the 2-amino group of substrate also is H-bonded to OE1 of Glu30. Consistent with the consensus for the reduction mechanisms of the natural substrates, folate and dihydrofolate, involving protonated forms,[8] the cationic (N3 protonated) form of the 8-methylpterin substrate is thought necessary to activate the C7 atom for subsequent transfer of a hydride ion from NADPH in the DHFR-catalyzed reaction,[4]

$$SH^+ + NADPH \rightarrow SH_2 + NADP^+ \qquad (1)$$

If the DHFR-catalyzed reduction of the 8-substituted pterins does indeed mimic reduction of the natural substrate folate,[4–6] the cationic form would be expected for the activated substrate in the enzyme. However, *ab initio* calculations of complexes in the gas phase suggest the neutral-pair form shown in Figure 1 is more stable, and even after including enzymic effects with a semiempirical QM/MM model, the perturbations due to the protein solvent environment appear insufficient to preferentially stabilize the normal cationic form.[9] However, due to the acidic nature of H3 in 8-substituted pterins, it is quite possible that a low-barrier hydrogen bond (LBHB) exists, especially when it is considered that the pK_a of the carboxylate group is estimated[9] to be about 4, i.e., reasonably close to that of 8-methylpterin (5.3[7]). Although apparently not a necessary condition for the existence of an LBHB,[10] other studies have shown that pK_a matching may be an important determining factor.[11] In addition, an LBHB generally appears to be associated with polar covalent bonds between the hydrogen atom and the two heteroatoms.[12,13] Thus, an LBHB formed between 8-methylpterin and the carboxyl group may be expected to retain much of the ionic character of the normally protonated substrate, thereby explaining the observation of cationic spectra for the DHFR-bound form of the N5-deaza inhibitor analogues[14] and activation toward hydride-ion transfer. These considerations and the results of the QM/MM studies[9] suggesting a small free energy gap favoring the neutral-pair form led us to perform calculations of the energetics of the transfer of the proton between the two potential minima.

If the system is an LBHB, the first vibrational level on the one-dimensional proton transfer coordinate lies very near or above the transition state. Electronically, this state would closely resemble the transition state for the proton transfer, as this is where the vibrational wavefunction has its maximum probability. The kinetic mechanisms for the normal H bond and LBHB cases are illustrated in Figure 2. In the normal H bond scheme, there are two distinct sets of vibrational states corresponding to protonated substrate bound to carboxylate ($E^-\cdots SH^+$) and unprotonated substrate bound to carboxylic acid ($EH\cdots S$) on the one-dimensional potential energy surface for the motion of the acidic proton. In this case, there exists a thermodynamic equilibrium between $E^-\cdots SH^+$ and $EH\cdots S$, but only the active form $E^-\cdots SH^+$ decays into products from hydride-ion transfer. In the case of an LBHB, there exists a single enzyme-bound state that must closely resemble the ion-pair ($E^-\cdots SH^+$) form to be activated for hydride-ion transfer.

In this article, we investigate whether the LBHB mode of binding is more likely for the 8-substituted class of substrates than the normal H-bonded forms. In principle, this minimum energy path could be obtained from a QM/MM calculation.

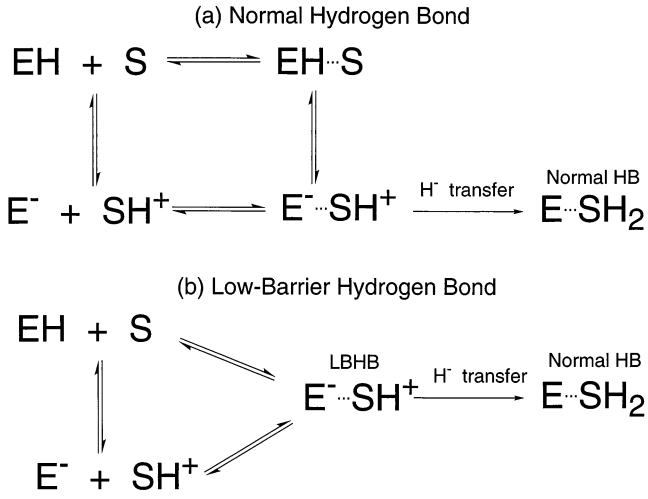

Figure 2. Kinetic schemes for (a) the normal ion-pair ($E^-\cdots SH^+$) and neutral-pair ($EH\cdots S$) forms of the H-bond interaction between substrate S and enzyme E, and (b) the low-barrier hydrogen bonded (LBHB) form.

However, although we have demonstrated that semiempirical QM/MM methods are capable of reproducing the free energies of interaction between a system and its environment,[15,16] they do not provide an accurate description of the H-bond characteristics of this system[9] or of proton motion in other H bonds.[11] Hence, we perform high-level QM calculations for an approximate continuum treatment of the enzyme using a number of self-consistent reaction field (SCRF) methods. The results of the SCRF calculations are first correlated with QM/MM calculations in order to determine an appropriate estimate of the effective dielectric constant for the protein. We then use the most appropriate SCRF method to generate the one-dimensional energy-optimized path for the transfer of the proton between the minima. Using this energy-optimized path together with harmonic vibrational frequencies, we confirmed the existence of an LBHB with characteristics consistent with experimental observations.

THEORY AND METHODS

Free Energy of Interaction

According to the normal H bonding scheme (Figure 2), the relative free energies of binding for the ion-pair ($E^-\cdots SH^+$) and neutral-pair ($EH\cdots S$) forms of the substrate-enzyme complex are given by

$$\Delta\Delta G_{bind} = \Delta E_{vacuum} + \Delta G_{int} + 2.3RT[pK_E - pK_S] \quad (2)$$

where ΔE_{vacuum} is the *ab initio* QM energy difference between the two H-bonded complexes (Figure 1) and ΔG_{int} is the difference in free energy for the interaction of the QM system with the protein/solvent environment. The remaining molecular constants are the acid dissociation constants of the protonated substrate (K_S) and the carboxylic acid sidechain of Asp or Glu in the enzyme active site (K_E). The free energy of interaction can be computed directly using MOPS[17] in an MD simulation using the coordinate-coupled free energy perturbation (FEP/MD) method

$$\Delta G_{int}(\mathbf{r},\mathbf{r} \pm \Delta\mathbf{r}) = -(RT)^{-1}\ln \times \langle \exp[-(E_{int}(r \pm \Delta r) - E_{int}(\mathbf{r}))/RT]\rangle_{\mathbf{r}} \quad (3)$$

where E_{int} is the interaction energy between the QM and MM systems.

If the protein/solvent environment, i.e., the MM part of the system in the QM/MM calculations, can be approximated as a continuous dielectric medium, the free energy difference of interaction also may be computed using the SCRF method. By definition the free energy, ΔG_{int} then is given by

$$\Delta G_{int} = \Delta E_{SCRF} - \Delta E_{vacuum} \quad (4)$$

Note, however, that ΔE_{SCRF} depends on the value of the dielectric constant (ϵ) of the medium, whereas ΔE_{vacuum} corresponds to $\epsilon = 1$. In order to model as accurately as possible the effects of the protein environment in the SCRF calculations, we have chosen a value for the dielectric constant that gives ΔG_{int} calculated via Equation 4 to be in close agreement with the FEP/MD result (Equation 3). In the present study, we model the Glu30 side chain by propionic acid to give $CH_3CH_2COO^-\cdots SH^+$ and $CH_3CH_2COOH\cdots S$ as the ion-pair and neutral-pair complexes, respectively. As there are several SCRF options available in Gaussian 98,[18] we initially calculated ΔG_{int} for these two complexes using the dielectric polarizable continuum model (DPCM),[19–21] integral equation formalism of PCM (IEFPCM),[22] isodensity surface PCM (IPCM),[23] conductor solvent model (COSMO),[24] and the Onsager equation[25] at the HF/6-31G* level. Note that even these more advanced SCRF models require some form of parameterization of atomic radii (DPCM, IEFPCM, COSMO) or other approximation (IPCM) for the size and shape of the molecular cavity. Where atomic radii were required as input (DPCM, IEFPCM, and COSMO), the default values in Gaussian 98 were used. The Onsager equation is particularly simple, as apart from the dielectric constant the only parameter is the cavity radius, which initially was estimated from a molecular volume calculation using Gaussian 98 to be 4.87 Å for the ion-pair complex and 5.23 Å for the neutral-pair complex.

QM/MM Calculations

The starting coordinates for the ternary complex consisting of DHFR, NADPH cofactor, and 8-methylpterin were based on the chicken liver DHFR.$NADP^+$.biopterin x-ray structure[26] as described in previous work.[27] The ternary complex including crystallographic water was solvated using a 34 Å shell containing approximately 3000 water molecules (approximately 12,000 atoms in total). We used the PM3 model[28] for the QM part of the system consisting of the substrate and side chain of the Glu30 residue (Figure 1) with the addition of a fluorine link atom[9] at the QM/MM interface. The interaction between the QM and MM systems contains electrostatic and van der Waals terms as described in previous work.[15,16] The molecular mechanics system consisting of the remaining protein and solvent was described using the united atom and all-atom force fields of Weiner et al.[29,30] and Cornell et al.[31] for the protein and the TIP3P force field[32] for water. For simulations with the Weiner et al. force fields, the all-atom force field[29] was used for protein residues within 8 Å of the substrate, with the remainder of the protein represented by the united-atom force field.[30] Due to the presence of charged amino acid groups in the enzyme, no cutoff was used for the QM/MM interactions. In order to obtain an improved description of the long-range electrostatic interactions for the MM parts of the systems, a 9 Å cutoff was imposed for all polar-polar residue and polar-charge residue interactions, while all interactions between charged residues were retained.

The MD simulations were carried out using the constant temperature algorithm of Berendsen et al.[33] with a minimum of 100 ps initial equilibration. In the coordinate-coupled FEP calculations (Equation 3), the distances $\{\mathbf{r}\}$ in Figure 1 were fixed using SHAKE[34] and the free energy change calculated at $\{\mathbf{r} \pm \Delta\mathbf{r}\}$ as the mean of plus and minus perturbations[9] over 20 intervals (windows) along the reaction coordinate with 3 ps each of equilibration and data collection per window, i.e., a total of 60ps after the initial equilibration. The free energy of interaction was calculated using both the Weiner et al. and Cornell et al. force fields and a final esimate of ΔG_{int} obtained by taking the mean value.

SCRF Proton-Transfer Path

An energy-optimized path for the proton motion is given by values of $\Delta E_{SCRF}(r)$, where r defines the one-dimensional reaction coordinate for the transfer of the acidic proton H3

between N3 and OE2 (Figure 1). We obtained this energy-optimized path by first fixing the distance r_1 = 0.95 Å and incrementing by 0.05 Å to a distance of 1.20 Å, at which point we switch to fixing the distance r_3 = 1.25 Å decreasing by 0.05 Å intervals to a distance of 0.95 Å. Similarly, we can start from the neutral pair configuration by fixing the distance r_3 = 0.95 Å with increments of 0.05 Å to a maximum of 1.25 Å, and then switch to fixing r_1 = 1.20 Å decreasing by 0.05 Å to 0.95 Å. At each fixed distance, r_3 or r_1, all the remaining geometrical parameters (a set of nonredundant internal coordinates) were optimized to the corresponding energy minimum. The energy-optimized path in vacuum was first generated at the HF/6-31G* level. However, it is well known that electron correlation is essential for the accurate determination of activation barriers. As SCRF gradients are not generally available at MP2 level, we performed single-point MP2/6-31G* calculations only on the HF/6-31G* path for different ϵ values. Also, as there are difficulties in computing accurate gradients in the more sophisticated SCRF methods, we used the Onsager model to generate the energy-optimized path. Consequently, in order to incorporate efficiently the effects of electron correlation and the dielectric medium in geometry optimizations for $\epsilon > 1$, we used the density functional (B3LYP) method[35,36] that is well suited for H-bonded systems,[37] together with the Onsager SCRF model.

RESULTS AND DISCUSSION

In Figure 3 we compare ΔG_{int} obtained from FEP/MD calculations using semiempirical (PM3) QM/MM force fields with that computed using *ab initio* HF/6-31G* SCRF methods. From the QM/MM calculations, we obtain −2.5 kcal/mol for the Weiner et al.[29,30] force field and −3.6 kcal/mol for the Cornell et al.[31] force field to give an estimate of $\Delta G_{int} = 3.1 \pm 0.5$ kcal/mol. The DPCM and IEFPCM methods give essentially the same result for ΔG_{int} for all dielectric constants. The IPCM method gives similar free energies to the DPCM and IEFPCM methods with the best agreement for low dielectric constants. For low dielectric constants, the COSMO and Onsager-1 results deviate from the DPCM, IEFPCM, and IPCM results. The Onsager-1 model is defined for a cavity radii of 4.87 Å for the ion-pair complex and 5.23 Å for the neutral-pair complex. For high dielectric constants, the difference between the DPCM and Onsager models becomes very large, while the corresponding difference between DPCM and COSMO results is small. For a dielectric constant of $\epsilon = 2$, the DPCM, IEFPCM, and IPCM results are consistent with the free energy of −3.1 kcal/mol obtained in the FEP/MD calculations, while the Onsager-1 and COSMO models give significantly higher ΔG_{int} values. However, we found that by changing the cavity radius in the Onsager equation to 5.5 Å for both ion-pair and neutral-pair complexes (referred to as the Onsager-2 model), excellent agreement with the DPCM and IEFPCM results also could be obtained. As the Onsager-2 model agrees well with the more sophisticated methods, it should be a useful tool for calculations on this system. Based on these results, we performed DPCM and Onsager-2 calculations on the energy-optimized path.

The HF/6-31G* energy-optimized path in vacuum ($\epsilon = 1$) for the transfer of H3 between the neutral-pair and ion-pair complexes (Figure 1) is shown in Figure 4. Also shown are the

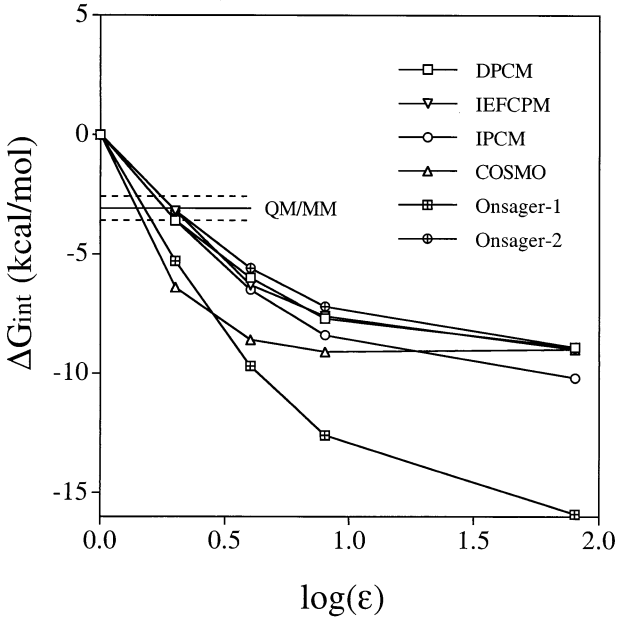

Figure 3. Free energy of interaction ΔG_{int} (kcal/mol) for various SCRF methods (see text) at the HF/6-31G level as a function of dielectric constant [log(ϵ)] compared with ΔG_{int} from QM/MM calculations. For Onsager-1, the cavity radius is 4.87 Å for the ion pair and 5.23 Å for the neutral pair. For Onsager-2, the cavity radius is 5.5 Å for both complexes.*

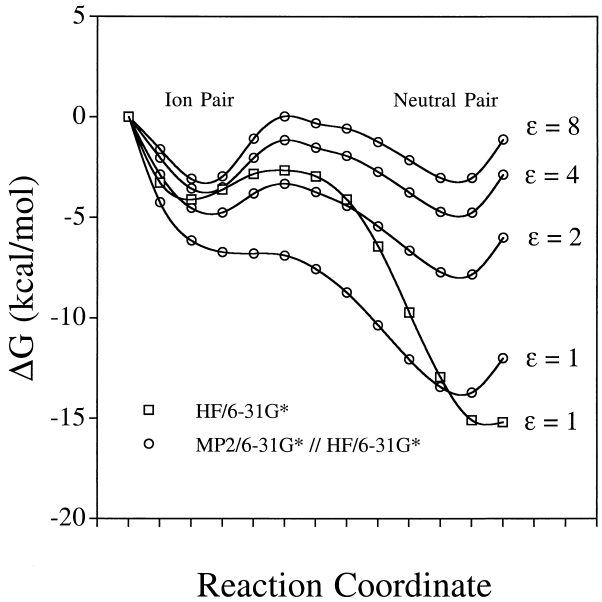

Figure 4. Single-point MP2/6-31G DPCM calculations for different values of the dielectric constant (ϵ = 1, 2, 4, 8) on the HF/6-31G* (ϵ = 1) energy-optimized path for the proton transfer reaction between 8-methylpterin substrate (S) and propionic acid (RCOOH). Note that in order to maintain the curves on the same scale, the energies are plotted relative to the first point on the path (set to zero).*

corresponding single-point MP2/6-31G* results generated for different values of the dielectric constant using the DPCM method. We found previously[9] that increasing the basis set size to 6-311+G** has only a minor effect on the energy difference between the minima, and that this energy difference is relatively insensitive to the level at which the geometries are optimized. The effect of correlation at the MP2 level is, as expected, to reduce the barrier to proton transfer. In fact, in vacuum the barrier for converting the ion pair to the neutral pair appears very small. It is likely that if optimizations were carried out at the MP2 level, the barrier would be zero. However, the dielectic effect ($\epsilon > 1$) of the environment clearly stabilizes the ion pair relative to the neutral pair and the barrier increases substantially. For dielectric constants between 4 and 8, the difference between the two minima is less than 1 kcal/mol with an activation barrier of about 3 kcal/mol. For $\epsilon = 2$, the neutral pair is 3 kcal/mol more stable than the ion pair. Coincidentally, this difference is the same as was found by the HF/6-31G calculations for the complexes in vacuum, as shown in Figure 5 together with the MP2 $\epsilon = 2$ pathway for comparison. At this lower level of theory, the vibrational frequencies can be readily calculated. On examination of the normal modes, we identified the N-H stretch in the ion pair at 2751 cm^{-1} and the O-H stretch in the neutral pair at 3153 cm^{-1} from which we obtain 3.9 and 4.5 kcal/mol, respectively, for the zero-point vibrational corrections. The position of the first vibrational level for the proton motion estimated using the 6-31G zero-point energy corrections can be seen to lie just above the TS. For these energy-optimized paths we would predict the existence of an LBHB.

It should be remembered, however, that the paths in Figures 4 and 5 were obtained by optimization at the HF level, starting from initial coordinates corresponding to the ion-pair and neutralpair complexes shown in Figure 1. We also carried out optimizations at the MP2/6-31G* level and although differences were minor in the region of the neutral pair, a significant change occurred in the ion-pair configuration. If the N-H3 distance in the ion-pair complex was reduced below the optimum MP2/6-31G* value[9] of about 1.10 Å, H2 of the substrate rapidly shifts to form a covalent bond with OE1 of the side chain and a H bond with N2 of the substrate. That is, the ion-pair complex converts to a second neutral-pair complex as shown in Figure 6. This transfer of H2 probably is facilitated at correlated levels by the general lowering of activation barriers. To check if this effect was an artifact of the method, we repeated the minimizations using B3LYP/6-31G* and B3LYP/6-31+G** density functional methods and obtained similar results, i.e., the minimum with the lower energy is this second neutral-pair complex.

Figure 7 shows the energy-optimized path generated at the B3LYP/6-31G* level and using the Onsager-2 equation (radius = 5.5 Å) to model the dielectric effects at $\epsilon = 2$. The minimum on the left-hand side of the TS corresponds to the second neutral-pair complex (Figure 6). Clearly, the ion pair also can be approached from this second minimum by moving H2 toward the 2-amino group of the substrate. Thus, the procedure for obtaining the energy-optimized path from the second neutral-pair complex was as described for the first neutral-pair complex except that r_2 and r_4 replace r_1 and r_3 as the fixed parameters. The first neutral-pair complex (Figure 1) is marginally (<0.5 kcal/mol) lower in energy. Based on the HF/6-31G ($\epsilon = 1$) O-H stretch frequency obtained for this

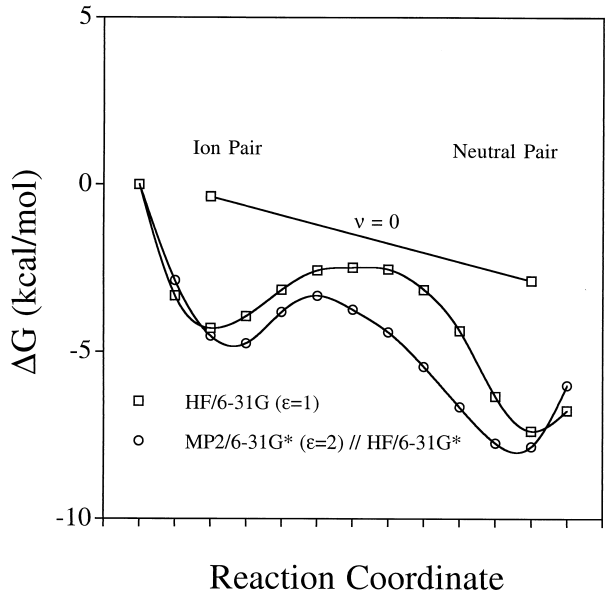

Figure 5. HF/6-31G ($\epsilon = 1$) energy-optimized path for the proton transfer reaction between 8-methylpterin substrate (S) and propionic acid (RCOOH). The estimated position of the first vibrational state ($\nu = 0$) is shown. The single-point MP2/6-31G DPCM ($\epsilon = 2$) curve from Figure 4 is shown for comparison.*

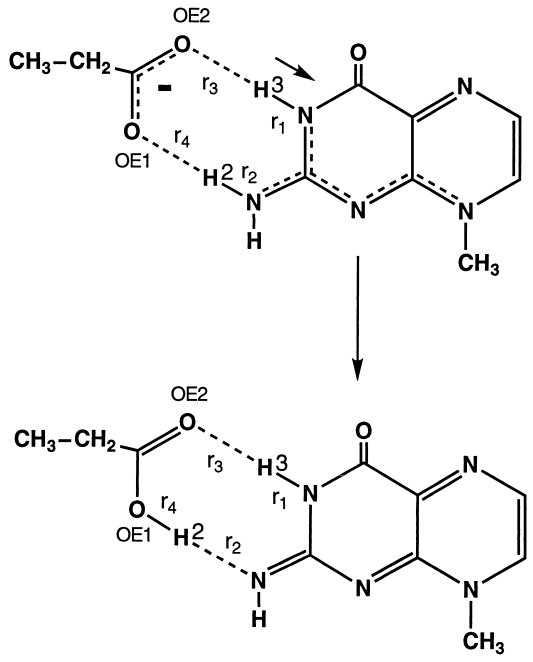

Figure 6. Change in H bonding between the 8-methylpterin substrate and carboxyl side chain from the ion-pair configuration to a stable alternative neutral-pair form resulting from compression (shown by arrow) of the N-H3 bond in geometry optimization carried out at the correlated (MP2 or B3LYP) level.

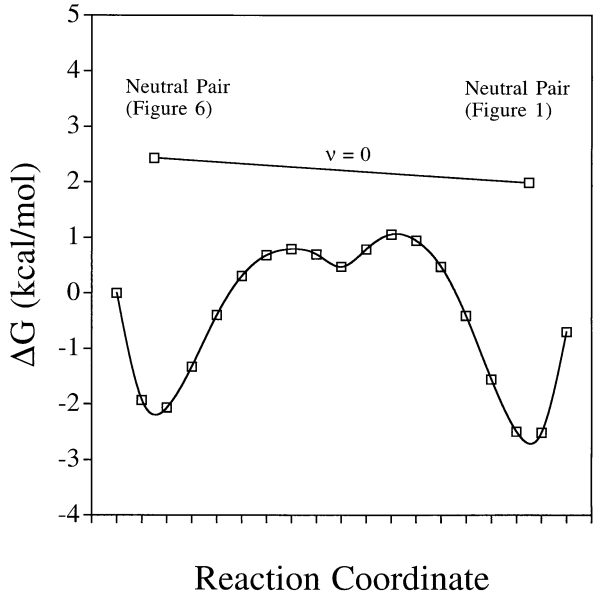

Figure 7. B3LYP/6-31G (ϵ = 2) energy-optimized path for the proton transfer reaction between 8-methylpterin substrate (S) and propionic acid (RCOOH). The estimated position of the first vibrational state (ν = 0) is shown. Onsager-2 equation (radius = 5.5 Å) was used for the SCRF model.*

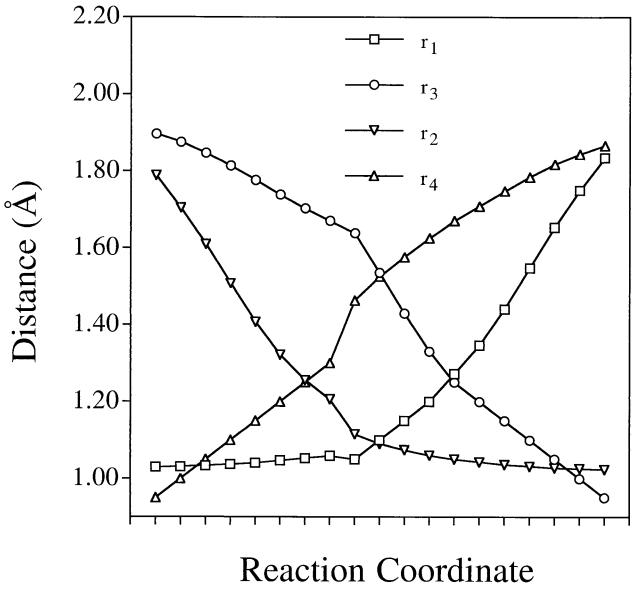

Figure 8. Distances (r_1, r_2, r_3, and r_4 in Figure 1) along the reaction coordinate computed at the B3LYP/6-31G (ϵ = 2) level for the energy-optimized path for proton transfer between the two neutral-pair forms shown in Figure 7. Onsager-2 equation (radius = 5.5 Å) was used for the SCRF model.*

neutral-pair complex (Figure 5), we estimate 4.5 kcal/mol for the zero-point energy correction. As this exceeds the 3.5 kcal/mol barrier for the proton transfer, we conclude that the system is an LBHB. However, given the uncertainties in the HF vibrational frequencies, the position of the zero-point level must be regarded as an estimate only. Hence, definite values cannot be attributed to the relative populations of the neutral and ion-pair forms. As the proton H3 moves further from OE2 in the first neutral-pair complex (Figure 1), we expect the complex becomes more like the ion pair. Similarly, the ion-pair complex starts to form on increasing the distance between H2 and OE1 in the second neutral-pair complex. The calculated dipole moment changes from approximately 10 D in the neutral-pair complexes to 15 D in the ion-pair complex, indicating a high degree of charge separation in the ion pair. The shift in the H bond geometry toward the ion-pair complex as the TS is approached from the minima can be seen from the interatomic distances r_1, r_2, r_3, and r_4, shown in Figure 8.

CONCLUSIONS

The QM/MM and SCRF calculations predict a lowering of the relative free energy in the enzyme but not to the extent that the ion-pair complex $E^{-}\cdots SH^{+}$ becomes thermodynamically more stable than the neutral pair complex $EH\cdots S$. The free energy for the interaction of the H-bonded system with the protein environment calculated using the QM/MM and FEP/MD methods corresponds most closely with results of *ab initio* HF/6-31G* SCRF calculations for a dielectric constant of 2. However, geometry optimizations at the correlated level show that the ion-pair complex is not even the second most stable configuration, but rather the second energy minimum corresponds to a second neutral-pair complex (Figure 6) with an energy only 0.5 kcal/mol above that of the first neutral pair (Figure 1) at the B3LYP/6-31G* (ϵ = 2) level. The activation barrier for the transfer of the two protons H3 and H2 between the two neutral-pair minima is approximately 3.5 kcal/mol at the B3LYP/6-31G* (ϵ = 2) level. The zero-point vibrational correction is estimated to be about 4.5 kcal/mol, indicating an LBHB. As the first vibrational level appears to lie near or above the two transition states (Figure 7), the H-bonded system will have a significant probability of being found in the state corresponding to the ion-pair complex, which is consistent with experimental spectral studies indicating an enzyme-bound cation.[14] Also, such a significantly cationic LBHB would activate substrate toward hydride-ion transfer from NADPH, consistent with the observed substrate activity of the 8-substituted pterins.[5,7]

ACKNOWLEDGMENTS

We gratefully acknowledge the Australian National University Supercomputer Facility for generous grants of computer time, and the support of an ANU Strategic Development Grant.

REFERENCES

1 Cummins, P.L., and Gready, J.E. Novel mechanism-based substrates of dihydrofolate reductase and the thermodynamics of ligand binding: A comparison of theory and experiment for 8-methylpterin and 6,8-dimethylpterin. *Prot. Struct. Funct. Genet.* 1993, **15**, 426–435

2 Cummins, P.L., and Gready, J.E. Molecular dynamics and free energy perturbation study of the hydride-ion transfer step in dihydrofolate reductase using a com-

bined quantum and molecular mechanical model. *J. Comput. Chem.* 1998, **19**, 977–988
3 Cummins, P.L., and Gready, J.E. Investigating enzyme reaction mechanisms with QM/MM+MD calculations. *ACS Symp. Ser.* 1998, **712**, 250–263
4 Gready, J.E. Theoretical studies on the activation of the pterin cofactor in the catalytic mechanism of dihydrofolate reductase. *Biochemistry* 1985, **24,** 4761–4766
5 Thibault, V., Koen, M.J., and Gready, J.E. Enzymic properties of a new mechanism-based substrate for dihydrofolate reductase. *Biochemistry* 1989, **28**, 6042–6049
6 Gready, J.E., Cummins, P.L., and Wormell P. Computer-aided design of mechanism-based pterin analogues and FEP/MD simulations of their binding to dihydrofolate reductase. *Adv. Exp. Med. Biol.* 1993, **338**, 487–492
7 Ivery, M.T.G., and Gready, J.E. Structure-activity relationships for the 8-alkylpterins: A new class of mechanism-based substrate for dihydrofolate reductase (DHFR) *Biochemistry* 1995, **34**, 3724–3733
8 Brown, K.A., and Kraut, J. Exploring the molecular mechanism of dihydrofolate reductase. *Faraday Discuss.* 1992, **93**, 217–224
9 Cummins, P.L., and Gready, J.E. Combined quantum and molecular mechanics (QM/MM) study of the ionization state of 8-methylpterin substrate bound to dihydrofolate reductase. *J. Phys. Chem.*, in press
10 Garciaviloca, M., Gonzalezlafont, A., and Lluch, J.M. On pKa matching as a requirement to form a low-barrier hydrogen bond: A theoretical study in the gas phase. *J. Phys. Chem.* 1997, **101**, 3880–3886
11 Chen, J.G., Mcallister, M.A., Lee, J.K., and Houk, K.N. Short, strong hydrogen bonds in the gas phase and in solution: Theoretical exploration of pKa matching and environmental effects on the strengths of hydrogen bonds and their potential roles in enzymatic catalysis. *J. Org. Chem.* 1998, **63**, 4611–4619
12 Schiott, B., Iversen, B.B., Madsen, G.K.H., Larsen, F.K., and Bruice, T.C. On the electronic nature of low-barrier hydrogen bonds in enzymatic reactions. *Proc. Natl. Acad. Sci. U.S.A.* 1998, **95**, 12799–12802
13 Schiott, B., Iversen, B.B., Madsen, G.K.H., and Bruice, T.C. Characterization of the short strong hydrogen bond in benzoylacetone by ab initio calculations and accurate diffraction experiments: Implications for the electronic nature of low-barrier hydrogen bonds in enzymatic reactions. *J. Am. Chem. Soc.* 1998, **120**, 12117–12124
14 Jeong, S.-S., and Gready, J.E. Ionization state and pK_a of pterin-analogue ligands bound to dihydrofolate reductase. *Eur. J. Biochem.* 1994, **221**, 1055–1062
15 Cummins, P.L., and Gready, J.E. Coupled semiempirical molecular orbital and molecular mechanics model (QM/MM) for organic molecules in aqueous solution. *J. Comput. Chem.* 1997, **18**, 1496–1512
16 Cummins, P.L., and Gready, J.E. Coupled semiempirical quantum mechanics and molecular mechanics (QM/MM) calculations on the aqueous solvation free energies of ionized molecules. *J. Comput. Chem.* 1999, **20**, 1028–1038
17 Cummins, P.L. *MOPS (Molecular Orbital Programs for Simulations).* Australian National University, Canberra, 1996
18 Frisch, M.J., Trucks, G.W., Schlegel, H.B., Scuseria, G.E., Robb, M.A., Cheeseman, J.R., Zakrzewski, V.G., Montgomery, J.A. Jr., Stratmann, R.E., Burant, J.C., Dapprich, S., Millam, J.M., Daniels, A.D., Kudin, K.N., Strain, M.C., Farkas, O., Tomasi, J., Barone, V., Cossi, M., Cammi, R., Mennucci, B., Pomelli, C., Adamo, C., Clifford, S., Ochterski, J., Petersson, G.A., Ayala, P.Y., Cui, Q., Morokuma, K., Malick, D.K., Rabuck, A.D., Raghavachari, K., Foresman, J.B., Cioslowski, J., Ortiz, J.V., Stefanov, B.B., Liu, G., Liashenko, A., Piskorz, P., Komaromi, I., Gomperts, R., Martin, R.L., Fox, D.J., Keith, T., Al-Laham, M.A., Peng, C.Y., Nanayakkara, A., Gonzalez, C., Challacombe, M., Gill, P.M.W., Johnson, B., Chen, W., Wong, M.W., Andres, J.L. Gonzalez, C., Head-Gordon, M., Replogle, E.S., and Pople, J.A. *Gaussian 98, Revision A.6.* Gaussian, Inc., Pittsburgh, PA, 1998
19 Miertus, S., Scrocco, E., and Tomasi, J. Electrostatic interaction of a solute with a continuum. A direct utilization of ab initio molecular potentials for the prevision of solvent effects. *Chem. Phys.* 1981, **55**, 117–129
20 Miertus, S., and Tomasi, J. Approximate evaluations of the electrostatic free energy and internal energy changes in solution processes.*Chem. Phys.* 1982, **65**, 239–245
21 Cossi, M., Barone, V., Cammi, R., and Tomasi, J. Ab initio study of solvated molecules: A new implementation of the polarizable continuum model. *Chem. Phys. Lett.* 1996, **255**, 327–335
22 Cances, M.T., Mennucci, V., and Tomasi, J. A new integral equation formalism for the polarizable continuum model: Theoretical background and applications to isotropic and anisotropic dielectrics. *J. Chem. Phys.* 1997, **107**, 3032–3041
23 Foresman, J.B., Keith, T.A., Wiberg, K.B., Snoonian J., and Frisch M.J. Solvent effects .5. Influence of cavity shape, truncation of electrostatics, and electron correlation ab initio reaction field calculations. *J. Phys. Chem.* 1996, **100**, 16098–16104
24 Barone, V., and Cossi, M. Quantum calculation of molecular energies and energy gradients in solution by a conductor solvent model.*J. Phys. Chem. A* 1998, **102**, 1995–2001
25 Onsager, L. Electric moments of molecules in liquids. *J. Am. Chem. Soc.* 1936, **58**, 1486
26 McTigue, M.A., Davies, J.F., Kaufman, B.T., and Kraut, J. Crystal structure of chicken liver dihydrofolate reductase complexed with $NADP^+$ and biopterin. *Biochemistry* 1992, **31**, 7264–7273
27 Cummins, P.L., and Gready, J.E. Solvent effects in active-site molecular dynamics simulations on the binding of 8-methyl-N5-deazapterin and 8-methylpterin to dihydrofolate reductase. *J. Comput. Chem.* 1996, **17**, 1598–1611
28 Stewart, J.J.P. Optimization of parameters for semiempirical methods II. Applications. *J. Comput. Chem.* 1989, **10,** 221–264
29 Weiner, S.J., Kollman, P.A., Case, D.A., Singh, U.C., Ghio, C., Alagona, G., Profeta, S., and Weiner, P.K. A new force field for molecular mechanical simulation of nucleic acids and proteins. *J. Am. Chem. Soc.* 1984, **106**, 765–784
30 Weiner, S.J., Kollman, P.A., Nguyen, D.T., and Case, D.A. An all atom force field for simulations of proteins and nucleic acids. *J. Comput. Chem.* 1986, **7**, 230–252
31 Cornell, W.D., Cieplak, P., Bayly, C.I., Gould, I.R., Merz K.M. Jr., Ferguson, D.M., Spellmeyer, D.C., Fox,

T., Caldwell, J.W., and Kollman, P.A. A second generation force field for the simulation of proteins, nucleic acids, and organic molecules. *J. Am. Chem. Soc*. 1995, **117**, 5179–5197
32 Jorgensen, W.L., Chandrasekhar, J., Madura, J.D., Impey, R.W., and Klein, M.L. Comparison of simple potential functions for simulating liquid water. *J. Chem. Phys.* 1983, **79**, 926–935
33 Berendsen, H.J.C., Postma, J.P.M., van Gunsteren, W.F., DiNola, A., and Haak, J.R. Molecular dynamics with coupling to an external bath *J. Chem. Phys.* 1984, **81**, 3684–3690
34 van Gunsteren, W.F., and Berendsen, H.J.C. Algorithms for macromolecular dynamics and constraint dynamics. *Mol. Phys.* 1977, **34**, 1311–1327
35 Lee, C., Yang, W., and Parr, R.G. Development of the Colle-Salvetti correlation energy formula into a functional of the electron density. *Phys. Rev. B* 1988, **37**, 785–789
36 Becke, A.D. Density-functional thermochemistry. III. The role of exact exchange. *J. Chem. Phys.* 1993, **98**, 5648–5652
37 Lozynski, M., Rusinskaroszak, D., and Mack, H.G. Hydrogen bonding and density functional calculations: The B3LYP approach as the shortest way to MP2 results. *J. Phys. Chem.* 1998, **102**, 2899–2903